厚生労働科学研究費補助金
医療技術実用化総合研究事業

RET融合遺伝子陽性の進行非小細胞肺癌に対する新規治療法の確立に関する研究

平成25年度　総括研究報告書

研究代表者　後藤　功一

平成26（2014）年　4月

厚生労働科学研究費補助金
医療技術実用化総合研究事業

RET融合遺伝子陽性の進行非小細胞肺癌に対する新規治療法の確立に関する研究

平成25年度　総括研究報告書

研究代表者　後藤　功一

平成26（2014）年　4月

目　　次

Ⅰ．総括研究報告

厚生労働科学研究費補助金（医療技術実用化総合研究事業）
（総括）研究報告書

RET 融合遺伝子陽性の進行非小細胞肺癌に対する新規治療法の確立に関する研究

研究代表者　後藤　功一
独立行政法人国立がん研究センター東病院
呼吸器内科外来医長

研究要旨

2012 年に発見された肺癌の新規ドライバー遺伝子である RET 融合遺伝子の臨床応用を目指した研究を実施した。RET 融合遺伝子陽性肺癌（RET 肺癌）は全肺癌の 1-2%と頻度が低いため、全国規模の遺伝子診断ネットワーク（LC-SCRUM-Japan）を立ち上げ、平成 25 年 2 月より遺伝子スクリーニングを開始した。同時に、RET 肺癌に対する Vandetanib の医師主導治験（LURET study）を世界で初めて開始した。平成 26 年 2 月 28 日現在、LC-SCRUM-Japan には 161 施設が参加し、602 例が登録された結果、RET 肺癌が 23 例スクリーニングされ、このうち 8 例が LURET study に登録されている。

研究分担者

葉　清隆	国立がん研究ｾﾝﾀｰ東病院	医員
河野隆志	国立がん研究ｾﾝﾀｰ研究所	分野長
蔦　幸治	国立がん研究ｾﾝﾀｰ中央病院	医長
土原一哉	国立がん研究ｾﾝﾀｰ東病院	分野長
石井源一郎	国立がん研究ｾﾝﾀｰ東病院	ﾕﾆｯﾄ長
松本慎吾	国立がん研究ｾﾝﾀｰ東病院	医師
大津　敦	国立がん研究ｾﾝﾀｰ	ｾﾝﾀｰ長
山中竹春	国立がん研究ｾﾝﾀｰ	室長
佐藤暁洋	国立がん研究ｾﾝﾀｰ	室長
大江裕一郎	国立がん研究ｾﾝﾀｰ東病院	副院長
田村友秀	国立がん研究ｾﾝﾀｰ中央病院	科長
村上晴泰	静岡がんセンター	医長
瀬戸貴司	九州がんセンター	医師
西尾誠人	がん研究会有明病院	部長
里内美弥子	兵庫県立がんセンター	部長
野上尚之	四国がんセンター	医長

A.　研究目的

希少疾患である RET 融合遺伝子陽性の進行非小細胞肺癌（RET 肺癌）を対象に、国内未承認の医薬品である RET チロシンキナーゼ阻害薬 Vandetanib（治験成分記号：ZD6474）の薬事承認申請を目指した多施設共同非無作為化非盲検第Ⅱ相試験（医師主導治験）を実施する。

B.　研究方法

RET 肺癌の頻度は、肺癌全体の 1-2%と非常に低いため、患者のスクリーニングが重要となる。このため、日本全体から多施設が参加する遺伝子診断ネットワークを構築し、この中で「RET 融合遺伝子等の低頻度の遺伝子変化陽性肺癌の臨床病理学的、分子生物学的特徴を明らかにするための前向き観察研究」に基づいて RET 肺癌のスクリーニングを行う。施設倫理委員会で本研究が承認された

施設のみ、遺伝子スクリーニングへの参加が可能とした。RET 融合遺伝子の診断は、国立がん研究センターで開発した RT-PCR 法、FISH 法を用いて行うこととし、この診断技術を株式会社エスアールエル（SRL）へ技術移管し、実際の臨床検体の遺伝子解析は SRL が行った。同時に Vandetanib の医師主導治験を 7 施設（国立がん研究センター東・中央病院、がん研有明病院、静岡がんセンター、兵庫県立がんセンター、四国がんセンター、九州がんセンター）で開始し、スクリーニングされた RET 肺癌は、医師主導治験へ登録して、Vandetanib の有効性を検討する方針とした。

医師主導治験である「RET 融合遺伝子陽性の局所進行/転移性非扁平上皮非小細胞肺癌患者を対象とした Vandetanib（ZD6474）の多施設共同非無作為化非盲検第Ⅱ相試験」（LURET study）のプライマリーエンドポイントは、奏効割合。セカンダリーエンドポイントは、無増悪生存期間、病勢制御割合、奏効期間、全生存期間、有害事象、前・後化学療法の有効性とした。予定登録数 17 例、登録期間 2 年、追跡期間 1 年であり、主な適格規準は、1)年齢 20 歳以上、2)扁平上皮癌以外の非小細胞肺癌、3)局所療法不能の III 期又は IV 期、4)RET 融合遺伝子陽性（RT-PCR 法及び FISH 法でいずれも陽性）、5)EGFR 遺伝子変異陰性、ALK 融合遺伝子陰性、6)1 レジメン以上の化学療法を実施後、7)PS=0-2、8)測定可能病変あり、9)主要臓器機能が保持、10)患者本人から文書による同意が必要とした。治療方法は、21 日を 1 コースとして、Vandetanib 300mg を 1 日 1 回朝食後に経口投与として、疾患の増悪、または許容できない毒性が認められるまで投与を継続することにした。Vandetanib（治験成分記号：ZD6474）は、治験薬提供者であるアストラゼネカ株式会社から無償提供され、治験薬の製造の記録、品質保証の記録も併せて提供される。医師主導治験への登録、モニタリング、安全性情報の管理、データセンター、統計解析については、国立がん研究センター 早期・探索臨床研究センター 臨床試験支援室において行うこととした。

倫理面への配慮としては、患者の人権保護のため、医師主導治験に関係するすべての研究者は、ヘルシンキ宣言、ICH Harmonized Tripartite Guidelines for Good Clinical Practice、「医薬品の臨床試験の実施の基準に関する省令」（平成 9 年厚生省令第 28 号）およびその改正、関連通知を遵守して本治験を実施する。医師主導治験を実施するにあたり、治験実施計画書、説明同意文書等の関連文書は事前に、「医薬品の臨床試験の実施の基準に関する省令」（平成 9 年厚生省令第 28 号）に規定する治験審査委員会の承認を取得した。患者への説明は、治験審査委員会で承認が得られた研究の内容、費用及び補償の有無、利益相反の有無等について記載された説明文書を用いて行い、登録前に充分な説明と理解に基づく自発的同意を本人より文書で得ることを規定した。また、医師主導治験が適正に行われていることを確保するため、中央モニタリングに加えて原資料との照合を行う施設訪問モニタリングをサンプリングにて実施することを規定した。監査は、アストラゼネカ社が行う。データマネージメントはデータセンターで行い、データの取り扱い上、患者氏名等直接個人が識別できる情報を用いず、かつデータベースのセキュリティを確保し、個人情報保護を厳守した。

更に、薬事承認後の実地診療における確実な患者選択のために、RET 融合遺伝子のコンパニオン診断薬の開発も同時に行うこととした。本研究では、RT-PCR 法、FISH 法を用いて遺伝子診断を行い、患者のスクリーニングを行うが、新鮮凍結検体から RNA の抽出が必要となる RT-PCR 法は、臨床現場では実施困難な場合が多いと予想されるため、ターゲットキャプチャー法を応用したゲノム DNA からの RET 融合遺伝子診断法の開発も同時に行った。このため、スクリーニングのために全国から収集した検体は保存し、今後のコンパニオン診断薬の開発のために二次利用することにした。

C. 研究結果

RET 肺癌のスクリーニングのため、全国規模の遺伝子診断ネットワークとして、Lung Cancer Genomic Screening Project for Individualized Medicine in Japan (LC-SCRUM-Japan)を組織し、平成 25 年 2 月 7 日より遺伝子スクリーニングを開始した。平成 26 年 2 月 28 日現在、LC-SCRUM-Japan には 161 施設が参加し、施設倫理審査委員会で研究が承認された 140 施設で順調に遺伝子スクリーニングが進行中である。平成 26 年 2 月 28 日までに LC-SCRUM-Japan には 602 例の登録があり、既に 23 例（4%）の RET 肺癌がスクリーニングされている。更に、希少な ROS1 融合遺伝子陽性肺癌 13 例(4%)、ALK 融合遺伝子陽性肺癌 13 例(4%)も同時にスクリーニングされている。

LURET study は、平成 24 年 11 月 19 日に PMDA の薬事戦略相談を受け、平成 25 年 1 月 29 日に治験計画届けを厚生労働省へ提出し、2 月 21 日より患者登録を開始した。平成 26 年 2 月 28 日までに LC-SCRUM-Japan でスクリーニングされた RET 肺癌 23 例のうち 8 例が LURET study に登録され、Vandetanib による治療が進行中であり、予想通りの治療効果が認められている。

これらと並行して、RET 融合遺伝子を含む複数の肺癌ドライバー変異を一度にかつ迅速に検出できるmultiplex 遺伝子診断法の開発も行っており、微量のゲノム DNA（50ng～）から、ターゲットキャプチャーを用いて目的ゲノム領域を濃縮し、次世

代シーケンサーで変異を検出するキットの開発が進行中である。これまでに既知の遺伝子変異をもつ約30の細胞株や臨床検体で正確に遺伝子変異の検出が可能であった。

D. 考察

肺癌はがん死亡原因第一位の難治性がんであり、2010年の年間死亡者数は約7万人で、がん死亡の約2割を占めている。非小細胞肺癌（主に腺癌、扁平上皮癌、大細胞癌）は、肺癌全体の約85%を占めるが、約2/3は発見時にすでに切除不能の進行癌であり、これらの患者に対しては化学療法が行われる。しかし、非小細胞肺癌は一般に化学療法の感受性が低く、現在の化学療法による治療成績は1年生存率が約40%と不良であり、非小細胞肺癌の治療成績の向上のためには優れた分子標的薬による個別化治療の推進が不可欠である。

近年、非小細胞肺癌における個別化治療の標的となる遺伝子異常（EGFR遺伝子変異、ALK融合遺伝子）が同定され、EGFR遺伝子変異例に対するEGFRチロシンキナーゼ阻害薬（ゲフィチニブ、エルロチニブ）や、ALK融合遺伝子陽性例に対するALKチロシンキナーゼ阻害薬（クリゾチニブ）の臨床応用によって、従来の化学療法と比較して、著しい治療成績の改善が認められている。

RET融合遺伝子は、2012年に報告された非小細胞肺癌の新しいドライバー遺伝子であり、新規の治療標的となることが期待される。RET肺癌は、肺癌全体の1-2%と頻度は低いが、基礎研究においてRETチロシンキナーゼ阻害薬であるVandetanibの有効性が確認されており、臨床試験に基づいたVandetanibの有効性の確認、早期臨床応用が期待されている。

Vandetanibはアストラゼネカ株式会社が開発中の国内未承認薬である。既に米国FDAでは、2011年4月に切除不能または進行性の甲状腺髄様癌に対する治療薬として承認されている。国内では、肺癌を含む固形がんを対象に第I相試験が行われ、推奨用量は海外と同じ300 mg/dayと設定され、更に、進行非小細胞肺癌に対する第II相試験において、主な有害事象は下痢、皮疹、高血圧、頭痛などで、これまでの報告とほぼ同じであり、安全性の確認は完了している。

RET肺癌は、頻度が1-2%という稀少疾患であるため、治療開発は医師主導治験以外では困難であり、Vandetanibの有効性を評価して薬事承認申請を目指す医師主導治験の実施が必須となる。このVandetanibの有効性を評価する本試験は、世界初の試みであると同時に、今後も明らかになる新たな遺伝子異常を伴う希少がんに対する分子標的治療薬の開発方法を考える上で、非常に重要な意味を持つと考えられる。

更に、本研究において、我が国初の全国規模の遺伝子診断ネットワークLC-SCRUM-Japanが構築され、希少肺癌のスクリーニングが成功したことは非常に重要である。少数施設で1-2%の頻度の希少な肺癌をスクリーニングして、新規治療法の開発を実施するのは不可能なため、希少肺癌では、従来とは異なる治療開発の方法が模索されてきた。本研究の中でLC-SCRUM-Japanという希少肺癌の遺伝子スクリーニング基盤が実際に構築されたことは大きな意義を持つと考えられる。また、希少肺癌の治療開発においては、正確な診断及び、スクリーニングが可能となるコンパニオン診断薬の同時開発が必須とされている。今後、LC-SCRUM-Japanは、遺伝子変化を伴うその他の希少肺癌のスクリーニングにも応用可能であり、また、全国から集めた多くの検体を利用し、multiplex診断薬を含めたコンパニオン診断薬の開発を担える組織として、更に存在意義が高まっていくと予想される。

E. 結論

本研究では、2012年に我が国で発見された肺癌の新規ドライバー遺伝子であるRET融合遺伝子の臨床応用を目指した研究を行っている。RET肺癌は希少頻度の肺癌であるが、全国規模の遺伝子診断ネットワークであるLC-SCRUM-Japanにおいて順調にスクリーニングが進行している。更に、スクリーニングされたRET肺癌は、Vandetanibの医師主導治験に登録され、治療開発も同時に進行している。このような民間企業の研究と公的資金に基づく医師主導治験との連携による治療開発システムの構築は、今後も明らかになる遺伝子異常を伴う希少がんに対する分子標的治療薬の効率的な治療開発のモデルケースとして注目されており、個別化治療の発展への大きな貢献が期待される。

F. 健康危険情報

なし

G. 研究発表

1. 論文発表

1. Suzuki T, Shibata T, Takaya K, Shiraishi K, Kohno T, Kunitoh H, Tsuta K, Furuta K, Goto K, Hosoda F, Sakamoto H, Motohashi H, Yamamoto M. Regulatory nexus of synthesis and degradation deciphers cellular Nrf2 expression levels. Mol Cell Biol, 2013, 33(12):2402-12.

2. Suzuki M, Makinoshima H, Matsumoto S, Suzuki A, Mimaki S, Matsushima K, Yoh K, Goto K, Suzuki Y, Ishii G, Ochiai A, Tsuta K, Shibata T, Kohno T, Esumi H, Tsuchihara K. Identification of a lung adenocarcinoma cell line with CCDC6-RET fusion

gene and the effect of RET inhibitors in vitro and in vivo. Cancer Sci, 2013, 104(7):896-903.

3. Suzuki A, Mimaki S, Yamane Y, Kawase A, Matsushima K, Suzuki M, Goto K, Sugano S, Esumi H, Suzuki Y, Tsuchihara K. Identification and characterization of cancer mutations in Japanese lung adenocarcinoma without sequencing of normal tissue counterparts. PLoS One, 2013, 8(9):e73484.

4. Kohno T, Tsuta K, Tsuchihara K, Nakaoku T, Yoh K, Goto K. RET fusion gene: translation to personalized lung cancer therapy. Cancer Sci. 2013, 104 (11): 1396-1400.

5. Yoshida A, Tsuta K, Wakai S, Arai Y, Asamura H, Shibata T, Furuta K, Kohno T, Kushima R. Immunohistochemical detection of ROS1 is useful for identifying ROS1 rearrangements in lung cancers. Mod Pathol. 2013[Epub ahead of print]

6. Arai Y, Totoki Y, Takahashi H, Nakamura H, Hama N, Kohno T, Tsuta K, Yoshida A, Asamura H, Mutoh M, Hosoda F, Tsuda H, Shibata T. Mouse model for ROS1-rearranged lung cancer. PLoS One. 2013,8(2):e56010.

7. Tsuta K, Kawago M, Inoue E, Yoshida A, Takahashi F, Sakurai H, Watanabe S, Takeuchi M, Furuta K, Asamura H, Tsuda H. The utility of the proposed IASLC/ATS/ERS lung adenocarcinoma subtypes for disease prognosis and correlation of driver gene alterations. Lung Cancer. 2013,81(3):371-6.

8. Ichinokawa H, Ishii G, Nagai K, Kawase A, Yoshida J, Nishimura M, Hishida T, Ogasawara N, Tsuchihara K, Ochiai A. Distinct clinicopathologic characteristics of lung mucinous adenocarcinoma with KRAS mutation. Hum Pathol. 2013,44:2636-42.

9. Bando H, Yoshino T, Shinozaki E, Nishina T, Yamazaki K, Yamaguchi K, Yuki S, Kajiura S, Fujii S, Yamanaka T, Tsuchihara K, Ohtsu A. Simultaneous identification of 36 mutations in KRAS codons 61and 146, BRAF, NRAS, and PIK3CA in a single reaction by multiplex assay kit. BMC Cancer. 2013,13:405.

H. 知的財産権の出願・登録状況

1. 特許取得
   知財(特許出願)
   なし
2. 実用新案登録
   なし
3. その他
   なし

Ⅱ．研究成果の刊行に関する一覧表

研究成果の刊行に関する一覧表

雑誌

発表者氏名	論文タイトル名	発表誌名	巻号	ページ	出版年
Suzuki T, Shibata T, Takaya K, Shiraishi K, Kohno T, Kunitoh H, Tsuta K, Furuta K, Goto K, Hosoda F, Sakamoto H, Motohashi H, Yamamoto M.	Regulatory nexus of synthesis and degradation deciphers cellular Nrf2 expression levels.	Mol Cell Biol.	33(12)	2402-12	2013
Suzuki M, Makinoshima H, Matsumoto S, Suzuki A, Mimaki S, Matsushima K, Yoh K, Goto K, Suzuki Y, Ishii G, Ochiai A, Tsuta K, Shibata T, Kohno T, Esumi H, Tsuchihara K.	Identification of a lung adenocarcinoma cell line with CCDC6-RET fusion gene and the effect of RET inhibitors in vitro and in vivo.	Cancer Sci.	104(7)	896-903	2013
Suzuki A, Mimaki S, Yamane Y, Kawase A, Matsushima K, Suzuki M, Goto K, Sugano S, Esumi H, Suzuki Y, Tsuchihara K.	Identification and characterization of cancer mutations in Japanese lung adenocarcinoma without sequencing of normal tissue counterparts.	PLoS One.	8(9)	e73484	2013
Kohno T, Tsuta K, Tsuchihara K, Nakaoku T, Yoh K, Goto K.	RET fusion gene: translation to personalized lung cancer therapy.	Cancer Sci.	104 (11)	1396-1400	2013

Yoshida A, Tsuta K, Wakai S, Arai Y, Asamura H, Shibata T, Furuta K, Kohno T, Kushima R.	Immunohistochemical detection of ROS1 is useful for identifying ROS1 rearrangements in lung cancers.	Mod Pathol.			[Epub ahead of print]
Arai Y, Totoki Y, Takahashi H, Nakamura H, Hama N, Kohno T, Tsuta K, Yoshida A, Asamura H, Mutoh M, Hosoda F, Tsuda H, Shibata T.	Mouse model for ROS1-rearranged lung cancer.	PLoS One.	8(2)	e56010	2013
Tsuta K, Kawago M, Inoue E, Yoshida A, Takahashi F, Sakurai H, Watanabe S, Takeuchi M, Furuta K, Asamura H, Tsuda H.	The utility of the proposed IASLC/ATS/ERS lung adenocarcinoma subtypes for disease prognosis and correlation of driver gene alterations.	Lung Cancer.	81(3)	371-6	2013
Ichinokawa H, Ishii G, Nagai K, Kawase A, Yoshida J, Nishimura M, Hishida T, Ogasawara N, Tsuchihara K, Ochiai A.	Distinct clinicopathologic characteristics of lung mucinous adenocarcinoma with KRAS mutation.	Hum Pathol.	44	2636-42	2013
Bando H, Yoshino T, Shinozaki E, Nishina T, Yamazaki K, Yamaguchi K, Yuki S, Kajiura S, Fujii S, Yamanaka T, Tsuchihara K, Ohtsu A.	Simultaneous identification of 36 mutations in KRAS codons 61and 146, BRAF, NRAS, and PIK3CA in a single reaction by multiplex assay kit.	BMC Cancer.	13	405	2013

Ⅲ. 研究成果の刊行物・別刷

研究代表者	後藤　功一	国立がん研究センター東病院
研究分担者	葉　　清隆	国立がん研究センター東病院
	河野　隆志	国立がん研究センター研究所
	蔦　　幸治	国立がん研究センター中央病院
	土原　一哉	国立がん研究センター東病院
	石井源一郎	国立がん研究センター東病院
	松本　慎吾	国立がん研究センター東病院
	大津　　敦	国立がん研究センター東病院
	山中　竹春	国立がん研究センター東病院
	佐藤　暁洋	国立がん研究センター東病院
	大江裕一郎	国立がん研究センター東病院
	田村　友秀	国立がん研究センター中央病院
	山本　信之	静岡がんセンター
	瀬戸　貴司	九州がんセンター
	西尾　誠人	がん研究会有明病院
	里内美弥子	兵庫県立がんセンター
	野上　尚之	四国がんセンター

MCB
Journals.ASM.org

Regulatory Nexus of Synthesis and Degradation Deciphers Cellular Nrf2 Expression Levels

Takafumi Suzuki,[a] Tatsuhiro Shibata,[b] Kai Takaya,[a] Kouya Shiraishi,[c] Takashi Kohno,[c] Hideo Kunitoh,[d] Koji Tsuta,[e] Koh Furuta,[e] Koichi Goto,[f] Fumie Hosoda,[b] Hiromi Sakamoto,[g] Hozumi Motohashi,[h] Masayuki Yamamoto[a,i]

Department of Medical Biochemistry[a] and Center for Radioisotope Sciences,[h] Tohoku University Graduate School of Medicine, and Tohoku Medical-Megabank Organization,[i] Sendai, Japan; Divisions of Cancer Genomics,[b] Genome Biology,[c] and Genetics,[g] National Cancer Center Research Institute, and Divisions of Pathology and Clinical Laboratories, National Cancer Center Hospital,[e] Tokyo, Japan; Department of Respiratory Medicine, Mitsui Memorial Hospital, Tokyo, Japan[d]; Division of Thoracic Oncology, National Cancer Center Hospital East, Kashiwa City, Chiba, Japan[f]

Transcription factor Nrf2 (NF-E2-related factor 2) is essential for oxidative and electrophilic stress responses. While it has been well characterized that Nrf2 activity is tightly regulated at the protein level through proteasomal degradation via Keap1 (Kelch-like ECH-associated protein 1)-mediated ubiquitination, not much attention has been paid to the supply side of Nrf2, especially regulation of *Nrf2* gene transcription. Here we report that manipulation of *Nrf2* transcription is effective in changing the final Nrf2 protein level and activity of cellular defense against oxidative stress even in the presence of Keap1 and under efficient Nrf2 degradation, determined using genetically engineered mouse models. In excellent agreement with this finding, we found that minor A/A homozygotes of a single nucleotide polymorphism (SNP) in the human *NRF2* upstream promoter region (rs6721961) exhibited significantly diminished *NRF2* gene expression and, consequently, an increased risk of lung cancer, especially those who had ever smoked. Our results support the notion that in addition to control over proteasomal degradation and derepression from degradation/repression, the transcriptional level of the *Nrf2* gene acts as another important regulatory point to define cellular Nrf2 levels. These results thus verify the critical importance of human SNPs that influence the levels of transcription of the *NRF2* gene for future personalized medicine.

The *Nrf2* (NF-E2-related factor 2; or *Nfe2l2*) gene encodes a basic leucine zipper-type transcription factor that belongs to the CNC (cap'n'collar) family (1). Nrf2 displays its transactivation activity through dimerization with one of the small Maf (sMaf) proteins, and the Nrf2-sMaf heterodimer recognizes a specific DNA sequence known as the antioxidant (ARE)/electrophile response element (EpRE) (2, 3). Downstream target genes of Nrf2 include enzymes that act in detoxifying and antioxidative stress responses, enzymes related to glutathione synthesis, and transporters, which together constitute a network to facilitate the cellular adaptation to oxidative and xenobiotic stresses (4, 43). Studies with the *Nrf2* gene knockout ($Nrf2^{-/-}$) mouse clearly demonstrate that Nrf2 deficiency attenuates the response to oxidative and electrophilic stresses (5, 6), resulting in high-level susceptibility to a variety of toxic chemicals and carcinogens (7–9). Similarly, Nrf2-deficient mice are prone to the initiation of carcinogenesis, demonstrating that Nrf2 contributes to cancer chemoprevention (10–12). Conversely, large numbers of cancer cells express high levels of Nrf2, and this fact indicates that cancer cells hijack and exploit Nrf2 activity for their malignant growth (13–15).

One of the important characteristics of Nrf2 is the inducible nature of its function in response to oxidative and electrophilic stresses (16). Under homeostatic and stress-free conditions, cellular Nrf2 abundance is maintained at a very low level, as the ubiquitin E3 ligase complex composed of Keap1 (Kelch-like ECH-associated protein 1) and cullin 3 specifically promotes ubiquitination and proteasomal degradation of Nrf2 (16, 44). Notably, Keap1 acts as a sensor for electrophilic and oxidative stresses by using reactive cysteine residues within the protein (17). Exposure to electrophiles or reactive oxygen species hampers Keap1 activity, reducing Nrf2 ubiquitination and leading to the stabilization and nuclear translocation/accumulation of Nrf2 (17). Subsequently, the expression of a battery of Nrf2 target genes is induced for cytoprotection against these insults. Thus, cellular Nrf2 activity is induced by a derepression mechanism utilizing the proteasomal protein degradation machinery (4).

Multiple lines of evidence support the mechanism of Nrf2 derepression from proteasomal degradation, which accounts for the inducible expression of Nrf2 target genes. On the contrary, changes in the supply side of Nrf2 seem to be less significant under these stress conditions than the derepression/accumulation mechanism of the Nrf2 protein (18). Thus, not much attention has been paid to the contribution of transcriptional regulation of the *Nrf2* gene to the accumulation of Nrf2 protein and inducible expression of its target genes. However, several lines of evidence suggest the importance of the transcriptional regulation of the *Nrf2* gene. For instance, the *Nrf2* mRNA level was found to increase approximately 2-fold 6 h after treatment of an electrophile in murine keratinocytes (19).

A promoter single nucleotide polymorphism (SNP) of the mouse *Nrf2* gene was found to be tightly linked to the sensitivity/

Received 16 January 2013 Returned for modification 31 January 2013
Accepted 1 April 2013
Published ahead of print 9 April 2013
Address correspondence to Masayuki Yamamoto, masiyamamoto@med.tohoku.ac.jp.
Takafumi Suzuki and Tatsuhiro Shibata contributed equally to this article.
Supplemental material for this article may be found at http://dx.doi.org/10.1128/MCB.00065-13.

doi:10.1128/MCB.00065-13

resistance of various inbred mouse lines to the toxicity of high concentrations (95%) of oxygen (8). Similarly, a variant of the *NRF2* gene in the upstream promoter region (rs6721961) (20) is associated with susceptibility to acute lung injury in humans (21). This human SNP is located in the middle of the ARE motif and weakens the affinity of NRF2 binding to the ARE. This regulatory SNP (rSNP) appears to disrupt the positive-feedback regulation of *NRF2* expression by NRF2 itself (21). Other consequences of this *NRF2* rSNP have also been reported, including the risk of venous thromboembolism (22), reduced vital capacity (23), and an impaired forearm vasodilator response (24).

However, it remains to be determined how significantly the *Nrf2* transcript level affects Nrf2 definitive activity *in vivo*. This is the most critical issue for the future use of this and related *NRF2* SNPs in risk assessment and personalized medicine. Therefore, to address this critical issue, we have exploited genetically engineered mouse models. Our present results unequivocally demonstrate the importance of the level of the Nrf2 supply in both the presence and absence of Keap1-mediated protein degradation regulation. In addition, in order to clarify how significantly the reduction of the *NRF2* mRNA level is linked to the pathogenesis of human diseases, we explored whether the *NRF2* rSNP rs6721961 contributes to the increased risk of non-small-cell lung carcinomas. We compared the incidence of each genotype of the *NRF2* rSNP in a lung cancer population and a control population. We also measured the endogenous expression of *NRF2* in immortalized lymphocytes. We found that the rSNP genotype indeed affects the *NRF2* mRNA level in peripheral lymphocytes and also brings about an increased risk of non-small-cell lung cancers. These results strongly argue that transcription of the *NRF2* gene is an important regulatory point for cellular NRF2 activity.

MATERIALS AND METHODS

Mice. *Nrf2*$^{-/-}$ and Keap1 gene knockout (*Keap1*$^{-/-}$) mice were produced and characterized as described previously (6, 25). Transgene construct *KRD*-Nrf2 was generated by subcloning the Flag-hemagglutinin (HA)-tagged mouse Nrf2 cDNA into the vector harboring a 5.7-kb *Keap1* gene regulatory domain (*KRD*) (26). Transgenic mice were generated as described previously (26). Four independent lines were established for *KRD*-Nrf2. All compound mutant mice examined in this study were from a mixed genetic background, with contributions from 129Sv/J, C57BL/6J, and ICR strains. For hematoxylin-eosin (H&E) staining, the esophagi of P10 pups or adult mice were fixed in 3.7% formalin and embedded in paraffin.

Cell culture. Peritoneal macrophages were isolated as described previously (5). Whole-cell extracts were prepared in a lysis buffer (26) and subjected to immunoblot analysis using anti-Nrf2 (27), anti-Flag (Sigma-Aldrich), anti-HA (Roche), and anti-α-tubulin (Sigma-Aldrich) antibodies. Cell viability after 1-chloro-2,4-dinitrobenzene (CDNB) treatment was determined using a Cell Counting Kit-8 (Dojin Laboratories) according to the manufacturer's protocol. Diethyl maleate (DEM) and CDNB were purchased from Wako Pure Chemicals. Menadione and benzyl isothiocyanate (BITC) were purchased from Sigma-Aldrich.

Real-time PCR. Total RNA was prepared from forestomachs or macrophages using an Isogen RNA extraction kit (Nippon Gene) or from immortalized lymphocytes using an RNeasy kit (Qiagen). The cDNAs were synthesized from the total RNA using SuperScript III reverse transcriptase (Invitrogen by Life Technology). Real-time quantitative PCR was performed using an ABI 7300 (Applied Biosystems by Life Technology) or LightCycler 480 (Roche) system. Primer and probe sequences are available upon request.

Study participants. All lung cancer cases and controls were Japanese. These cases received treatments at the National Cancer Center Hospitals (NCCH), Japan, from 2000 to 2008. All surgically collected lung cancer specimens were pathologically examined by at least two board-certified pathologists in the NCCH. Histological diagnosis is based on the WHO classification of lung tumors (28). The controls were volunteers enrolled at the NCCH and at Keio University, located in Tokyo, Japan, with the following inclusion criteria: they could not have lung or other cancers or a history of cancer. All cases and controls, all of whom provided informed consent, were consecutively included in this study without any exclusion criteria. This study was approved by the institutional review boards of the National Cancer Center. Smoking habit was expressed by the number of pack-years, which was defined as the number of cigarette packs smoked daily multiplied by the number of years of smoking. Those who had never smoked (never smokers) were defined as individuals for whom the number of pack-years was 0. Those who had ever smoked (ever smokers) were defined as individuals for whom the number of pack-years was >0 and included both former and current smokers.

SNP analysis. Genomic DNA was extracted from whole blood from lung cancer cases and controls enrolled in the NCCH. Genomic DNA was extracted from Epstein-Barr virus-transformed B lymphocytes derived from whole blood collected from volunteers enrolled at Keio University. Genomic DNA was extracted using a blood maxikit or a QIAamp DNA minikit (Qiagen). The genotypes of NRF2 rSNP rs6721961 (referred to here as NRF2 rSNP-617) were determined by TaqMan SNP genotyping assays (Applied Biosystems by Life Technology).

Detection of somatic *EGFR* and *KRAS* mutations in lung tumors. Tumor samples were obtained at the time of surgery, rapidly frozen in liquid nitrogen, and stored at −80°C. Genomic DNA from the tissues was extracted using a QIAamp DNA minikit (Qiagen). Somatic mutations in the *EGFR* and *KRAS* genes were examined by high-resolution melting analysis (HRMA) as previously described (29).

Statistical analysis. Odds ratios (ORs) and 95% confidence intervals (CIs) for lung adenocarcinoma (ADC) risk were calculated after adjusting for gender, age (≤49, 50 to 59, 60 to 69, and ≥70 years), and smoking (never smoker versus ever smoker) by unconditional logistic regression analysis. These analyses were performed using JMP (version 8.0) software (SAS Institute Inc., Cary, NC).

RESULTS

Reflection of *Nrf2* gene dosage on cellular Nrf2 activity. To clarify how significantly reduction of *Nrf2* synthesis affects Nrf2 activity *in vivo*, we decided to exploit genetically engineered mouse models and examine whether transcriptional regulation of the *Nrf2* gene makes a substantial contribution to Nrf2 activity. Because Keap1 represses Nrf2 activity by accelerating the proteasomal degradation of the Nrf2 protein, a *Keap1*-null background provides an ideal model to analyze the gene dosage effect of *Nrf2*. Importantly, in this model system we can ignore the influence of Nrf2 degradation provoked by the Keap1-based ubiquitination of Nrf2. Indeed, *Keap1* gene knockout results in the constitutive accumulation of Nrf2, and the *Keap1*-null background is lethal in pups due to severe hyperkeratosis of the upper digestive tract (25). These phenotypes of the *Keap1*-null mice can be restored by simultaneous deletion of the *Nrf2* gene, indicating that the *Keap1*-null phenotype is attributable to the hyperactivation of Nrf2 (25).

When we deleted the *Nrf2* gene heterozygously in Keap1-deficient (i.e., *Keap1*$^{-/-}$::*Nrf2*$^{+/-}$) mice, we found a partial rescue of the severe phenotype of *Keap1*-null mice in the compound mutant mice. In contrast to the *Keap1*-null (*Keap1*$^{-/-}$::*Nrf2*$^{+/+}$) mice, the *Keap1*$^{-/-}$::*Nrf2*$^{+/-}$ mice survived to adulthood, as was the case for *Keap1*-null mice with the complete knockout of Nrf2 (*Keap1*$^{-/-}$::*Nrf2*$^{-/-}$). This indicates that deletion of a single allele

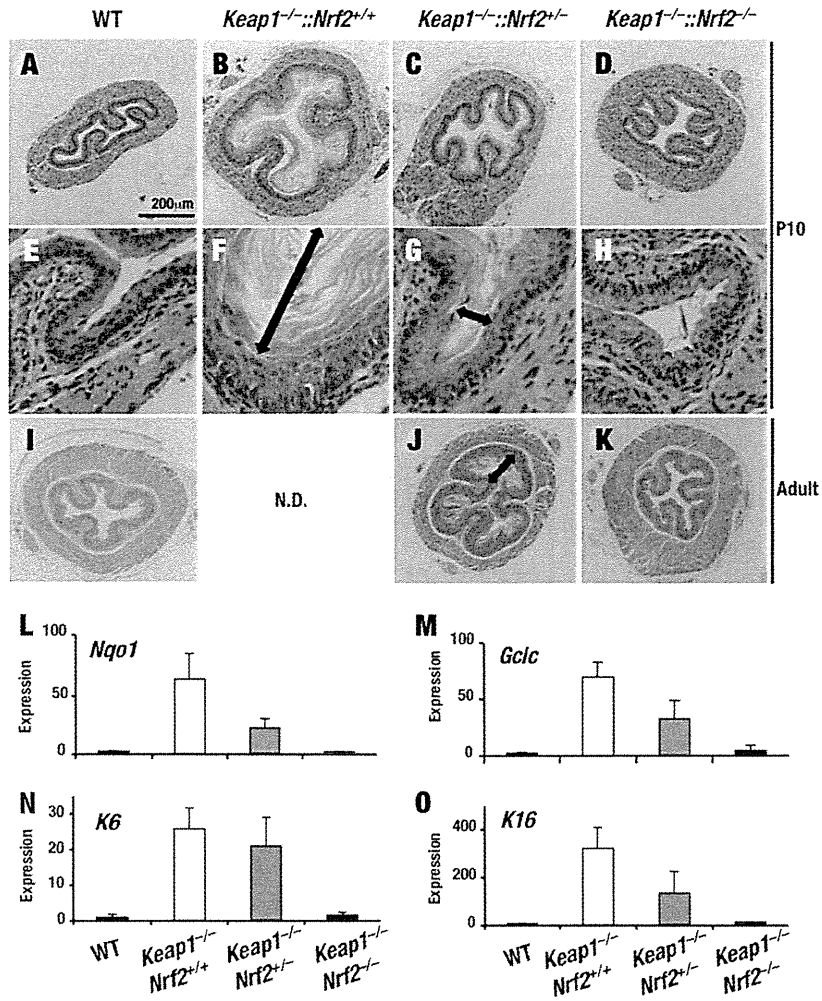

FIG 1 Heterozygous deletion of the *Nrf2* gene alleviates lethal phenotypes of Keap1-deficient mice. (A to K) H&E staining of transverse sections of the esophagus from P10 (A to H) and adult (I to K) mice. Lower (A to D) and higher (E to H) magnifications of the pictures are shown. Arrows indicate the thickened cornified layer. (L to O) Relative expression levels of the *Nqo1*, *Gclc*, *K6*, and *K16* genes compared with the level of 18S rRNA gene expression in the forestomachs of P10 mice. Data are the means ± SDs ($n = 3$). WT, wild type; N.D., no data.

of the *Nrf2* gene is sufficient to rescue the lethality caused by the Keap1 deficiency. We found that the average body weight of the *Keap1*$^{-/-}$::*Nrf2*$^{+/-}$ mice was less than that of the *Keap1*$^{-/-}$::*Nrf2*$^{-/-}$ mice in both males and females (see Fig. S1A and B in the supplemental material). Consistent with our previous observations (25), the *Keap1*$^{-/-}$::*Nrf2*$^{+/+}$ mice showed severe thickening of the cornified layers in the esophagus at 10 days after birth (Fig. 1B and F). On the contrary, the *Keap1*$^{-/-}$::*Nrf2*$^{+/-}$ mice showed clear improvement in the cornification and thickening (Fig. 1C and G). In adult *Keap1*$^{-/-}$::*Nrf2*$^{+/-}$ mouse esophagi, however, the thickening of the cornified layer became apparent (Fig. 1J). These results thus demonstrate that while the Nrf2 level synthesized from a single allele contributes to the esophageal phenotype to a certain extent in the *Keap1* knockout background (*Keap1*$^{-/-}$::*Nrf2*$^{+/-}$), it gives rise to a phenotype much milder than that resulting from the Nrf2 level synthesized from two alleles in the *Nrf2* wild-type background (*Keap1*$^{-/-}$::*Nrf2*$^{+/+}$).

Consistent with the esophageal phenotypes, the levels of expression of Nrf2 target genes, such as *Nqo1* [NAD(P)H:quinone oxidoreductase 1] and *Gclc* (glutamate-cysteine ligase catalytic subunit), and keratin-related genes, including *K6* (keratin 6) and *K16* (keratin 16), were lower in the forestomachs of *Keap1*$^{-/-}$::*Nrf2*$^{+/-}$ mice than in those of *Keap1*$^{-/-}$::*Nrf2*$^{+/+}$ mice but were higher than those in the forestomachs of *Keap1*$^{-/-}$::*Nrf2*$^{-/-}$ mice (Fig. 1L to O). Specifically, the levels of expression in the forestomachs of *Keap1*$^{-/-}$::*Nrf2*$^{+/-}$ mice were approximately half of the levels in *Keap1*$^{-/-}$::*Nrf2*$^{+/+}$ mice, indicating the presence of haploinsufficiency in *Nrf2* gene expression. These results thus indicate that the *Nrf2* gene dosage has an impact on Nrf2 activity *in vivo*.

Nrf2 synthesis is a critical determinant of cytoprotection capacity. Our next question was whether the Nrf2 transcription level affects the cellular capacity of cytoprotection even in the presence of Keap1-mediated Nrf2 degradation. To this end, we adopted thioglycolate-elicited mouse peritoneal macrophages as an experimental system, as this peritoneal macrophage system is well established as a system for testing the roles played by Nrf2 in the stress response (5). We first confirmed that in Nrf2 heterozygous

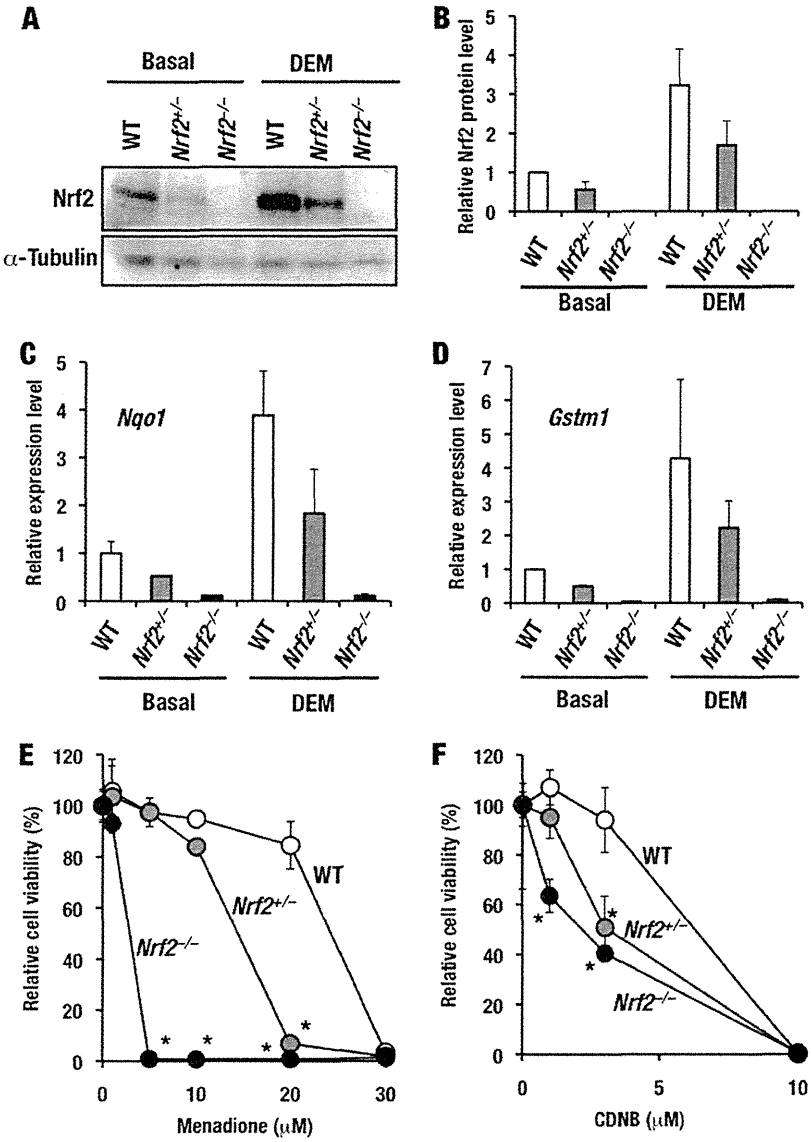

FIG 2 Heterozygous deletion of the *Nrf2* gene attenuates the ultimate activity of Nrf2 and impairs the oxidative stress response. (A) The Nrf2 protein level in macrophages from wild-type, $Nrf2^{+/-}$, and $Nrf2^{-/-}$ mice during the basal and DEM-induced states. (B) A graphical representation of the results in panel A is shown. Data are the means ± SDs ($n = 3$). (C and D) Relative *Nqo1* (C) and *Gstm1* (D) expression levels compared with the level of 18S rRNA gene expression of macrophages from wild-type, $Nrf2^{+/-}$, and $Nrf2^{-/-}$ mice under basal and DEM-induced conditions. Data are the means ± SDs ($n = 3$). (E and F) Relative viability of macrophages from wild-type, $Nrf2^{+/-}$, and $Nrf2^{-/-}$ mice after 12 h of treatment with menadione (E) or CDNB (F). *, statistical significance compared with the result for wild-type cells ($P < 0.05$). Data are the means ± SDs ($n = 3$).

($Nrf2^{+/-}$) macrophages the *Nrf2* transcript level was almost half of that in wild-type cells (see Fig. S2A in the supplemental material), corresponding to the allele number difference in the *Nrf2* gene. Since Nrf2 is constitutively degraded in the basal state, we expected that in Nrf2 heterozygous cells the Nrf2 protein level would not change significantly from the wild-type level under normal conditions. To our surprise, however, the Nrf2 protein level in $Nrf2^{+/-}$ macrophages was clearly decreased compared with that in wild-type cells under basal conditions (Fig. 2A and B). When cells were stimulated with DEM, an electrophilic Nrf2 inducer, the Nrf2 protein level in $Nrf2^{+/-}$ cells became almost half of that in wild-type cells. Consistent with the Nrf2 protein level, the *Nqo1* and *Gstm1* (glutathione *S*-transferase, mu 1) mRNA level was significantly reduced under both basal and induced conditions (Fig. 2C and D). These results suggest that gene dosage does influence cellular Nrf2 activity and cytoprotection under both basal and induced conditions.

To test whether the decrease in the *Nrf2* allele reduces cytoprotective functions, we examined whether $Nrf2^{+/-}$ macrophages are more susceptible to the cytotoxic effect of xenobiotics than wild-type cells. We employed menadione, CDNB, and BITC, which are well-established stressors for testing the roles played by Nrf2 in the stress response (30). Consistent with the reduced expression of *Nqo1* and *Gstm1* in Nrf2 heterozy-

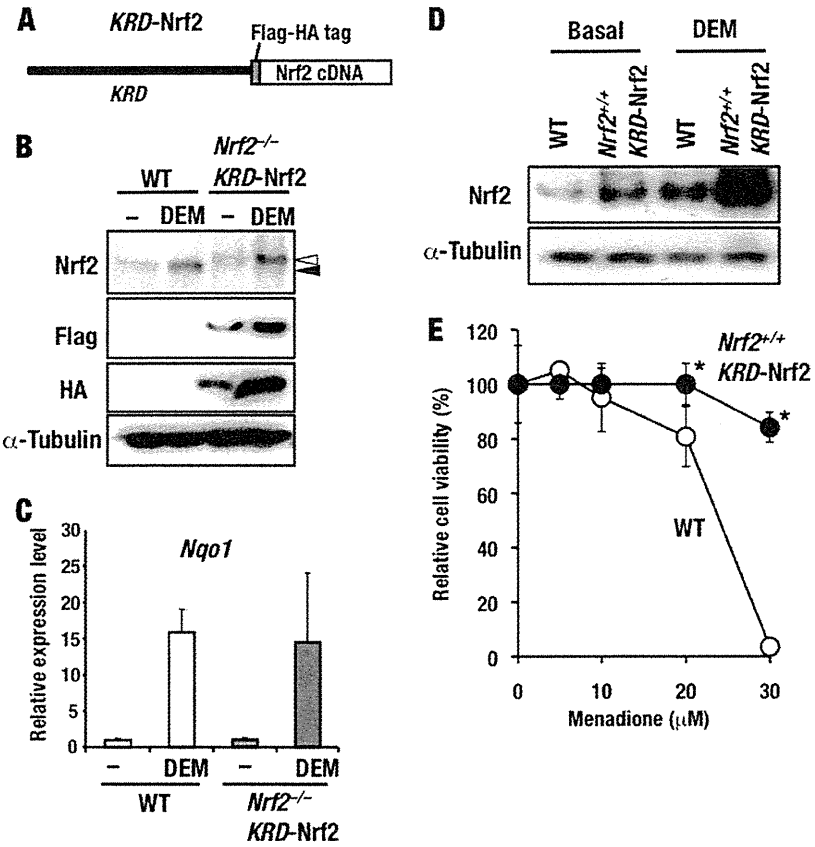

FIG 3 Increase in Nrf2 synthesis enhances Nrf2 activity and makes cells resistant to oxidative stress. (A) Structure of the transgene *KRD*-Nrf2. The Flag-HA double tag was fused to the N terminus of mouse Nrf2, and the fusion protein was expressed under the regulation of the Keap1 regulatory domain (*KRD*). (B) Level of transgene-derived Nrf2 expression in macrophages from *Nrf2*$^{-/-}$::*KRD*-Nrf2 mice. Closed and open arrowheads, endogenous Nrf2 and transgene-derived Flag-HA tagged Nrf2, respectively. (C) Relative levels of *Nqo1* expression compared with 18S rRNA gene expression in macrophages in the basal and DEM-induced states. Data are the means ± SDs ($n = 3$). (D) Nrf2 protein level in macrophages from wild-type and *Nrf2*$^{+/-}$::*KRD*-Nrf2 mice in the basal and DEM-induced states. Note the increase in the Nrf2 protein level in basal and DEM-treated *Nrf2*$^{+/-}$::*KRD*-Nrf2 macrophages. (E) Relative viability of macrophages from wild-type and *Nrf2*$^{+/+}$::*KRD*-Nrf2 mice after 12 h of treatment with menadione. Data are the means ± SDs ($n = 3$). *, statistical significance compared with the result for wild-type cells ($P < 0.05$).

gous macrophages, the cells appeared to be more susceptible to menadione, CDNB, and BITC than the wild-type cells but less susceptible to the insult than Nrf2-null macrophages (Fig. 2E and F; see Fig. S3 in the supplemental material), showing the haploinsufficiency of the *Nrf2* gene. These results thus demonstrate that the *Nrf2* mRNA expression level is critical for protecting cells from a wide range of xenobiotics.

Elevation of Nrf2 synthesis makes cells resistant to oxidative stress. *Keap1* gene knockout in mice results in an increase in Nrf2 protein levels. However, how the increase in *Nrf2* mRNA levels influences Nrf2 protein levels and cytoprotection is unclear. To assess the influence of *Nrf2* mRNA induction, we generated transgenic mouse lines that expressed Flag-HA-tagged Nrf2 under the control of the *Keap1* gene regulatory domain (*KRD*-Nrf2) (26) (Fig. 3A). Four independent lines were established for the *KRD*-Nrf2 transgene. We first examined whether transgene-derived Nrf2 protein was functional by crossing the transgenic mice with *Nrf2*-null mice (*Nrf2*$^{-/-}$::*KRD*-Nrf2). The transgenic mouse line expressed the transgene-derived Nrf2 protein at a level comparable to that of endogenous Nrf2 in macrophages under the basal and DEM-induced conditions (Fig. 3B), although the transgene-derived transcript was much more abundant than the endogenous Nrf2 transcript (see Fig. S2B in the supplemental material). This result is most likely due to the limited efficiency of translation from the transgene-derived mRNA, but the reasons for this are unknown. *Nqo1* expression was increased in the presence of DEM in *Nrf2*$^{-/-}$::*KRD*-Nrf2 macrophages to an extent similar to that in wild-type macrophages (Fig. 3C), indicating that the transgene-derived Nrf2 activated its target gene in response to DEM as efficiently as endogenous Nrf2.

We next analyzed the *KRD*-Nrf2 mice in the wild-type background (*Nrf2*$^{+/+}$::*KRD*-Nrf2). The Nrf2 protein level was robustly increased in the macrophages of *Nrf2*$^{+/+}$::*KRD*-Nrf2 mice compared with that in wild-type macrophages, irrespective of the induction status (Fig. 3D). When challenged with menadione, *Nrf2*$^{+/+}$::*KRD*-Nrf2 macrophages were more resistant to the cytotoxic effect of a high concentration of menadione than the wild-type control (Fig. 3E). Thus, although previous analyses argued that Nrf2 accumulated within the cells due to the derepression of rapid proteasome-dependent degradation, our present results demonstrate that the increase in *Nrf2* synthesis also effectively contributes to the increase in total cellular Nrf2 activity. Collectively, regulation of syn-

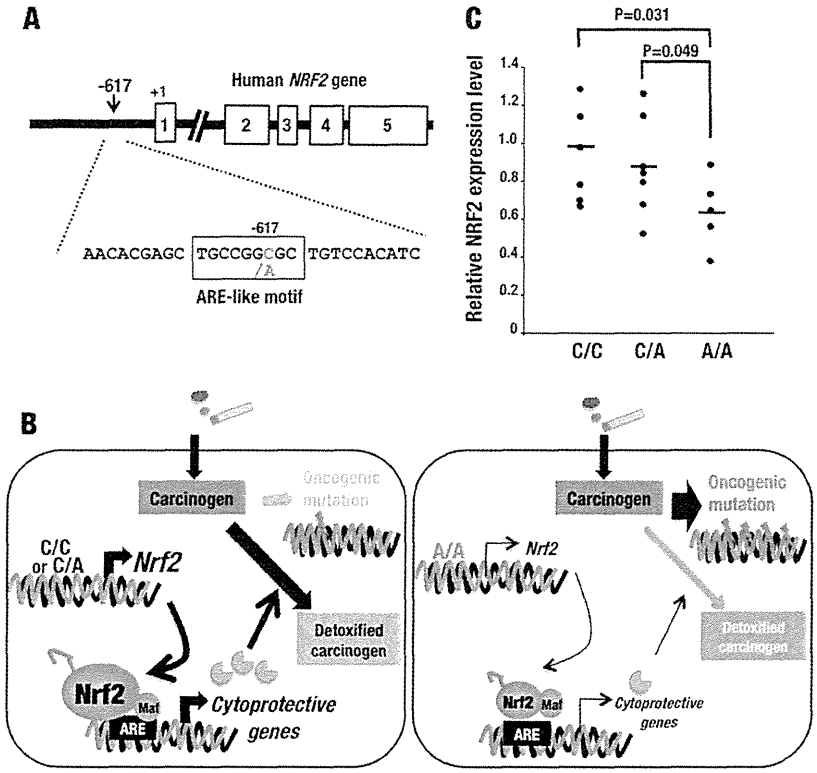

FIG 4 Genotypes of NRF2 rSNP-617 that affect *NRF2* gene expression. (A) Location of NRF2 rSNP-617 in the *NRF2* gene locus. The five exons are indicated by the numbered boxes. NRF2 rSNP-617 is located in the ARE-like motif in the promoter region of the *NRF2* gene. The polymorphic nucleotides are shown in red. (B) Schematic presentation of the putative mechanism for the association of NRF2 rSNP-617 and an increased risk of lung cancer. A/A homozygotes for NRF2 rSNP-617 significantly exhibit decreased expression of the *NRF2* gene and its downstream cytoprotective genes, resulting in the impaired detoxification of tobacco carcinogens and frequent oncogenic events. (C) Relative levels of human *NRF2* gene expression compared with *GAPDH* gene expression in immortalized lymphocytes of three different genotypes of NRF2 rSNP-617.

thesis and degradation in combination determines the cellular Nrf2 levels under basal and induced conditions.

Association of *NRF2* SNP and lung cancer susceptibility. Analyses of mouse models revealed that weakened transcription of the *Nrf2* gene results in the reduction of Nrf2 activity. We surmise that this reduction of NRF2 activity due to an *NRF2* SNP and reduced *NRF2* mRNA expression underlies various disease susceptibilities and/or pathophysiologies in humans. Therefore, we decided to examine the association of the *NRF2* SNP and lung cancer susceptibility.

A few SNPs within the *NRF2* gene have been described (20, 21). Of these SNPs, we focused on SNP rs6721961, located 617 bp upstream from the transcription start site of the gene (Fig. 4A), in this study. This SNP has been reported to be associated with the risk of acute lung injury (21), and its minor allele frequency varies among populations, as shown by the HapMap and 1,000 Genomes Projects (http://www.ncbi.nlm.nih.gov/projects/SNP/snp_ref.cgi?rs=6721961). We refer to rSNP rs6721961 as NRF2 rSNP-617 in this study. We conducted a case-control study consisting of 2,701 lung cancer patients (1,987 patients with ADC, 411 patients with squamous cell carcinoma [SQC], and 303 patients with small-cell lung carcinoma [SCC]) and 1,167 controls who had distributions of age, gender, ethnicity, and smoking status similar to those of the patient population (Table 1). All 3,868 case and control subjects were genotyped for the NRF2 rSNP-617, and the association of the genotypes with the risk for development of lung cancers was examined (Table 2). Notably, the frequency of the minor allele (i.e., the A allele, which causes a low level of expression, as described below) for this SNP was more prevalent in lung cancer patients than in controls (Table 2). Homozygotes for the minor allele (A/A) and the recessive mode (A/A homozygotes versus C/A heterozygotes plus C/C homozygotes) for the minor allele showed significant associations with overall lung cancer risk (odds ratio [OR] = 1.54 [$P = 0.0084$] and OR = 1.53 [$P = 0.0083$], respectively).

We next examined the association of NRF2 rSNP-617 with lung cancer risk according to clinicopathological factors. Minor homozygotes showed similarly increased risks for all histological types of lung cancers, including ADC, SQC, and SCC (Table 2). The homozygotes showed a higher risk in ever smokers than in never smokers (OR = 2.57 [$P = 0.00041$] versus OR = 1.13 [$P = 0.58$]) (Table 2).

We further examined the association of NRF2 rSNP-617 with the risk for developing lung ADC according to oncogenic pathway, i.e., *EGFR* and *KRAS* driver gene mutations (31) (Table 3). Minor homozygotes showed similarly increased risks for both lung ADC-bearing *EGFR* and *KRAS* mutations, with the association of ADC with the *EGFR* mutation being significant due to a large number of subjects (OR = 1.55 [$P = 0.0497$] and OR = 1.39 [$P = 0.47$], respectively). In contrast, an increase in the OR was

TABLE 1 Profiles of lung cancer cases and control cases that were analyzed in this study

Variable	Controls	Cases[a]						
			ADC					
				Mutation status				
		All	All	*EGFR*	*KRAS*	None	SQC	SCC
Total no. of cases	1,167	2,701	1,987	600	114	489	411	303
Mean ± SD age (yr)	49 ± 11	59 ± 11	58 ± 11	59 ± 10	59 ± 8	58 ± 10	61 ± 8	62 ± 11
No. (%) of subjects of the following sex:								
Male	725 (62)	1,746 (65)	1,137 (57)	243 (41)	81 (71)	315 (64)	366 (89)	243 (80)
Female	442 (38)	955 (35)	850 (43)	357 (59)	33 (29)	174 (36)	45 (11)	60 (20)
No. (%) of subjects with the following smoking status:								
Never smoker	760 (65)	884 (33)	853 (43)	361 (60)	30 (26)	192 (39)	17 (4)	14 (5)
Ever smoker	407 (35)	1,817 (67)	1,134 (57)	239 (40)	84 (74)	297 (61)	394 (96)	289 (95)

[a] ADC, adenocarcinoma; SQC, squamous cell carcinoma; SCC, small-cell carcinoma.

not evident for lung ADC without *EGFR* and *KRAS* mutations (OR = 1.14, $P = 0.61$). These results therefore indicate that minor homozygotes (A/A) of the NRF2 rSNP-617 are associated with the risk for lung cancers, especially ever smokers (Fig. 4B). Notably, in lung ADC cases, the association was evident in cancers harboring *EGFR* mutations.

NRF2 rSNP-617 affects gene expression in lymphocytes. The NRF2 rSNP-617 coincides with the ARE motif, which is important

TABLE 2 Genotype distribution for the rs6721961 SNP between controls and cancer cases

Category[a]	Genotype	No. (%) of subjects		Adjusted OR (95% CI)	*P*
		Controls	Cancer cases		
All	C/C	627 (53.7)	1,466 (54.3)	Reference	
	C/A	477 (40.9)	1,026 (38.0)	1.02 (0.87–1.19)	0.85[b]
	A/A	63 (5.4)	209 (7.7)	1.54 (1.12–2.16)	0.0084[b]
	Dominant			1.08 (0.92–1.26)	0.34[b]
	Recessive			1.53 (1.11–2.12)	0.0083[b]
ADC	C/C		1,071 (53.9)	Reference	
	C/A		761 (38.3)	1.02 (0.87–1.21)	0.77[b]
	A/A		155 (7.8)	1.55 (1.12–2.18)	0.0088[b]
	Dominant			1.09 (0.93–1.27)	0.30[b]
	Recessive			1.53 (1.11–2.13)	0.0092[b]
SQC	C/C		230 (56.0)	Reference	
	C/A		149 (36.3)	0.89 (0.66–1.21)	0.46[b]
	A/A		32 (7.8)	2.05 (1.11–3.85)	0.023[b]
	Dominant			1.00 (0.75–1.33)	0.99[b]
	Recessive			2.19 (1.18–4.12)	0.013[b]
SCC	C/C		165 (54.5)	Reference	
	C/A		116 (38.3)	1.00 (0.72–1.39)	0.99[b]
	A/A		22 (7.3)	1.82 (0.91–3.68)	0.092[b]
	Dominant			1.08 (0.79–1.48)	0.63[b]
	Recessive			1.83 (0.93–3.61)	0.082[b]
Never smoker	C/C	408 (53.7)	476 (53.8)	Reference	
	C/A	302 (40.0)	344 (39.0)	1.12 (0.89–1.41)	0.33[c]
	A/A	50 (6.6)	64 (7.2)	1.19 (0.77–1.83)	0.44[c]
	Dominant			1.13 (0.91–1.41)	0.26[c]
	Recessive			1.13 (0.74–1.73)	0.58[c]
Ever smoker	C/C	219 (53.8)	990 (54.5)	Reference	
	C/A	175 (43.0)	682 (37.5)	0.94 (0.75–1.18)	0.58[c]
	A/A	13 (3.2)	145 (8.0)	2.48 (1.42–4.70)	8.9×10^{-4}[c]
	Dominant			1.05 (0.84–1.31)	0.68[c]
	Recessive			2.57 (1.49–4.86)	4.1×10^{-4}[c]

[a] ADC, adenocarcinoma; SQC, squamous cell carcinoma; SCC, small-cell carcinoma.
[b] Adjusted for sex, age, and smoking status.
[c] Adjusted for sex and age.

TABLE 3 Association of the rs6721961 SNP and risk for development of lung ADC with or without the *EGFR* or *KRAS* mutation

Category	Genotype	No. (%) of subjects		Adjusted OR[a] (95% CI)	*P*
		Controls	Cancer cases		
EGFR mutation	C/C	627 (53.7)	327 (54.5)	Reference	
	C/A	477 (40.9)	224 (37.3)	1.00 (0.80–1.25)	1.00
	A/A	63 (5.4)	49 (8.2)	1.55 (1.00–2.38)	0.0497
	Dominant			1.07 (0.86–1.32)	0.56
	Recessive			1.55 (1.01–2.36)	0.044
KRAS mutation	C/C		63 (55.3)	Reference	
	C/A		44 (38.6)	0.95 (0.62–1.44)	0.80
	A/A		7 (6.1)	1.39 (0.54–3.10)	0.47
	Dominant			0.99 (0.66–1.48)	0.97
	Recessive			1.55 (0.61–3.44)	0.33
None	C/C		273 (55.8)	Reference	
	C/A		190 (38.9)	0.99 (0.78–1.25)	0.95
	A/A		26 (5.3)	1.14 (0.68–1.90)	0.61
	Dominant			1.00 (0.80–1.26)	0.95
	Recessive			1.14 (0.68–1.87)	0.61

[a] Adjusted for sex, age, and smoking status.

for *NRF2* expression in a feed-forward activation mechanism. Because the A allele-containing ARE is mutated, the transcription level of the *NRF2* gene is expected to be lower in the A allele case than in the C allele case, but no conclusive answer to whether the NRF2 rSNP-617 affects transcription of the *NRF2* gene *in vivo* has been obtained. To address this issue, we quantified the *NRF2* mRNA in immortalized human lymphocytes with distinct NRF2 rSNP-617 genotypes (Fig. 4C). We found that the *NRF2* mRNA levels were significantly lower in A/A homozygotes than in C/A heterozygotes and C/C homozygotes by approximately 40% ($P = 0.031$ and 0.049, respectively). No significant difference was observed between C/C homozygotes and C/A heterozygotes ($P = 0.47$), indicating that a homozygous nucleotide change from C to A at NRF2 rSNP-617 significantly decreased *NRF2* mRNA expression. Consistent with the NRF2 mRNA level, the levels of expression of *tert*-butylhydroquinone-induced NRF2 protein (see Fig. S4 in the supplemental material) and *NQO1* mRNA (see Fig. S5 in the supplemental material) were lower in A/A homozygote than in C/C genotype lymphocytes. These results strongly support the notion that the level of *NRF2* gene transcription is important for the role of NRF2 in cytoprotection, including cancer prevention (Fig. 4B).

DISCUSSION

In this study, we showed clinical and experimental lines of evidence that the final Nrf2 protein level in cells is under dual regulation at the protein degradation level and gene transcription level. The characteristic phenotypes of *Keap1*-null mice, i.e., hyperkeratosis and growth retardation, which are attributable to high Nrf2 activity, are significantly improved by deletion of a single allele of the *Nrf2* gene. Under physiological conditions (in the presence of Keap1-dependent Nrf2 degradation), a decrease in the *Nrf2* mRNA level markedly attenuates the final Nrf2 protein level, which in turn increases the susceptibility of mice to a wide range of xenobiotics. Conversely, when the Nrf2 mRNA level is increased, the Nrf2 protein level is enhanced and the cellular defense against oxidative stress is augmented. In excellent agreement with these results, we found that minor A/A homozygotes of NRF2 rSNP-617 exhibit significantly decreased *NRF2* gene expression and, consequently, increased the risk of lung cancers, especially in ever smokers. Thus, as summarized in Fig. 5, coordinated synthesis and degradation of Nrf2 are critically important for the maintenance of cellular redox homeostasis. Of note, we verified in this study that the transcription level of the *NRF2* gene is indeed important for the roles that NRF2 plays in cytoprotection.

The experiments utilizing genetically engineered mice demonstrate that a decrease in the *Nrf2* transcript to approximately half of its level is physiologically critical. This observation supports the contention that minor A/A homozygotes of NRF2 rSNP-617 are susceptible to lung cancers because of the 40% reduction in the *NRF2* transcript. Notably, changes in *Nrf2* transcript level alter the Nrf2 protein level, even in the basal state, in which Keap1 actively degrades Nrf2. This observation has led us to consider the kinetic properties of Keap1-dependent degradation of Nrf2. We surmise two possible models here. One is the threshold model, in which the Keap1-based ubiquitin E3 ligase system degrades Nrf2 efficiently and completely if its abundance is below a certain threshold. The other is the probability model, in which the Keap1-based ubiquitin ligase system degrades a certain ratio of Nrf2 irrespective of its abundance. Our present results support the latter model, as the status of Nrf2 synthesis exquisitely reflects the Nrf2 protein level, especially under basal conditions.

The analysis of lung cancer patient cohort and non-cancer patient populations revealed that NRF2 rSNP-617 has an association with susceptibility to lung cancer, especially for ever smokers. Although smoking is the top-ranked risk factor for lung cancer, little is known about genetic variations that increase the cancer risk related to smoking. Previous large-scale genome-wide association studies revealed the associations between variations in the nicotine receptor gene (32, 33) or the CYP1A1 and CYP2A6 detoxification enzyme genes (34) and susceptibility in smoking-associated lung cancers. Because oxidative stress has been well established to be one of the main factors in smoking-associated carcinogenesis, the result of our clinical study is in very good agreement with the function of Nrf2 as a key regulator of the cellular response against oxidative stresses.